



## Natural Fiber Reinforced Polyurethane Rigid Foam

Sibel DEMİROĞLU<sup>1</sup>, Fatma ERDOĞAN<sup>2</sup>, Ecem AKIN<sup>3</sup>, Hüseyin Ata KARAVANA<sup>4</sup>, M. Özgür SEYDİBEYOĞLU<sup>5\*</sup>

<sup>1</sup>Nanotechnology Graduate Programme, İzmir Katip Çelebi University, İzmir, Turkey

<sup>2</sup>Department of Materials Science and Engineering, Faculty of Engineering, Ege University, İzmir, Turkey

<sup>3</sup>Biocomposite Engineering, Faculty of Interdisciplinary Sciences, İzmir Katip Çelebi University, İzmir, Turkey

<sup>4</sup>Department of Leather Engineering, Faculty of Engineering, Ege University, İzmir, Turkey

<sup>5</sup>Department of Materials Science and Engineering, Faculty of Engineering and Architecture, İzmir Katip Çelebi University, İzmir, Turkey

### Article Info

Received: 08/09/2016

Revision: 09/12/2016

Accepted: 04/04/2017

### Keywords

Bio-based polyurethane foam  
Biocomposites,  
Biofibers  
Mechanical strength  
Thermal properties

### Abstract

The main objective of this study was to prepare polyurethane foam reinforced with local Turkish natural resources. In this work, olive kernel and nutshell fibers were used for reinforcing the polyurethane foam. In order to characterize reinforced polyurethane samples, mechanical, chemical, thermal, and morphological methods were used. Mechanical properties of polyurethane foam were measured by compression test. With compression test, it was observed that compressive strength of polyurethane foam was increased with 2.5 wt % olive kernel. Functional groups of polyurethane foams were determined by Fourier Transform Infrared Spectroscopy. Thermal behavior of polyurethane foam was analyzed with thermogravimetric analyzer device. Among biocomposites, polyurethane foam filled with nutshell indicated higher thermal degradation than polyurethane foam filled with olive kernel. Scanning electron microscopy observations revealed that foam structure was formed with biofiber addition.

## 1. INTRODUCTION

Polyurethane (PU), is defined as a polymer containing urethane group, and has extensive application areas such as automotive, coatings, insulation, pillows, and biomedical, many other uses [1]. Polyurethane reaction is a step-growth polymerization reaction of diisocyanate with polyether polyols to produce polymers [2]. Polyurethane was used in 1937 first time by Otto Bayern [3]. It was followed by the flexible polyurethane foams in 1953 and then the rigid polyurethane in 1957 [4]. Rigid PU foams are formed by reacting polymeric methylene diphenyl diisocyanate and polyether polyols and are extremely cross-linked polymers [5, 6]. Rigid PU foams are generally utilized for insulation because they have thermal conductivity, low density, and moisture permeability properties [7].

Polyurethane foams are light, comfortable and durable. That's why, they can be applied in the fabrication of materials for different uses such as carpet underlay, automotive, furniture, packing and biomedical. In industry, polyurethane foams are modified by using fillers and to change properties such as density, dimensional stability and retraction from the mold [8, 9].

Today, the use of polyurethane foams is rising at a rapid rate because of their light weight, excellent strength to weight ratio, and comfort features [10]. Bio-based PU materials and PU foams are growing with expanding applications in many sectors such as automotive [11].

The use of bio-based resources instead of petroleum based materials is of great importance for the materials industry in the world to create environment friendly and sustainable materials. Polyurethane production from renewable resources has become a good alternative because of low cost and readily available. Renewable products such as biofibers are used in the reinforcement of rigid PU foams. In recent years,

there is a trend to make PU foams using biobased materials such as flax, hemp, starch, sugar cane and wood flour [12, 13]. These biofibers used as a reinforcing material in the matrix are seen to improve the mechanical properties i.e. increases PU compressive strength [13, 14]. Adding fibers increased compressive strengths of PU foam while decreased thermal stability of foam [15, 16].

In this current work, polyurethane foams reinforced with nutshell and olive kernel fibers were characterized by means of mechanical and thermal methods. In addition, neat polyurethane foam was produced to study the role of the bio-based fillers on the performance of the polyurethane foam. Consequently, morphology, thermal and mechanical properties of PU are discussed. To our knowledge, this is the first work to while nutshell and olive kernel in polyurethane foam preparation that is a side product in Turkey.

## 2. MATERIAL AND METHOD

### 2.1. Materials

In this study, polyether polyol and polymeric methylene diisocyanate (PMDI) were taken from BASF firm (Elastapor H2011/4 and IsoPMDI 92140). Ratio of used polyol-PMDI was 100/102 in the study. The viscosity of polyol is 396 mPa s and viscosity of isocyanate is 270 mPa s. (100 rpm, 25 °C). The values of density and viscosity of raw materials are shown in Table 1. Nutshell was taken from Ordu city of Turkey and olive kernel supplied from İzmir, Turkey.

**Table 1.** Properties of polyol and isocyanate raw

	Unit	Polyol	Isocyanate
Density (25 °C)	g cm <sup>-3</sup>	1.13	1.23
Viscosity (25 °C)	mPa s	396	270

### 2.2. Production method

Production step of polyurethane foam are pictured in Figure 1.

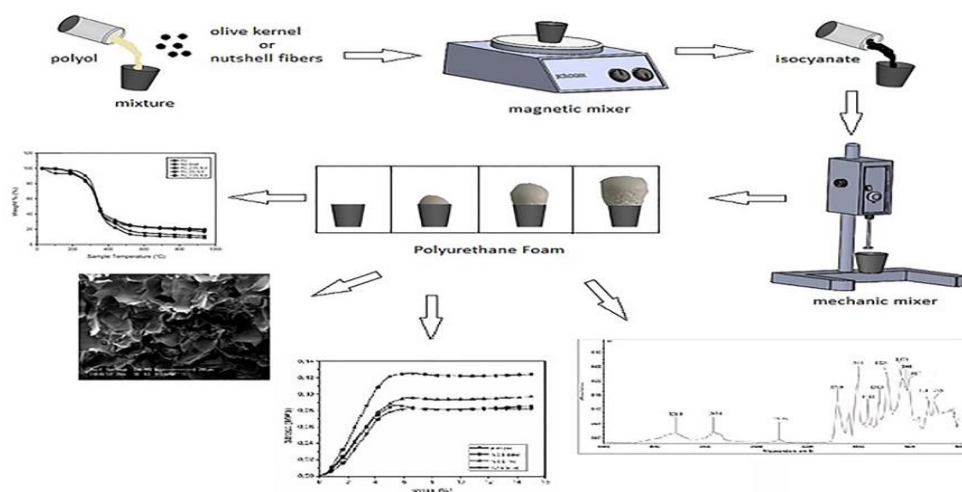


**Figure 1.** Presentment of experimental steps for PU study

The amount of biofiber, polyol, and isocyanate were prepared on the assay balance. (Denver Instrument). Two component system was used in PU producing. First of all, biofiber and polyol were mixed, then

isocyanate was added to get a reaction. Polyol and fiber were mixed in the magnetic mixer for 15 minutes (IKA C-MAG HS 7). Biofibers were homogeneously distributed in the polyol. After that, isocyanate was added into the biofiber and polyol mixture. Mechanical mixer was used to get homogenous mixture and PU foam. The mixture was mixed at 600 rpm for 20 seconds.

## **2.3 Characterization methods**

### **2.3.1 Particle Size**

Nutshells and olive kernels were ground to powder form, via vibratory disc mill, then mesh analysis of the powder was performed using 200 mesh. Particle size of the powders measured using Mastersizer 2000 Malvern device via laser scattering method.

### **2.3.2 X-Ray diffraction (XRD) analysis**

Nutshells and olive kernel samples were used for X-ray diffraction analysis. X-ray diffraction analysis was performed on a Bruker D2 Phaser system with Ni-filtered Cu-K alpha radiation ( $k = 1.54 \text{ \AA}$ ). The scanning  $2\theta$  angle of the X-ray diffraction analyses was recorded between  $5^\circ$  and  $80^\circ$ . The step time and the increment were 0.05 and 0.024 sec, respectively.

### **2.3.3 Thermogravimetric analysis (TGA)**

The TGA analysis was performed in the temperature from  $30^\circ\text{C}$  to  $950^\circ\text{C}$  by Perkin Elmer Diamond TG/DTA. The measurements were done with a heating rate of  $10^\circ\text{C min}^{-1}$  under nitrogen atmosphere. The analysis was utilized to determine weight loss rate when the polymer was heated up to  $950^\circ\text{C}$ .

### **2.3.4 Fourier Transform Infrared (FTIR) spectroscopy**

Structural characterization of different natural fiber reinforced PU foam was realized with Thermo Scientific, model Nicoletta IS5 with ATR mode. The analysis was done in the spectral range of  $500\text{--}4000 \text{ cm}^{-1}$  with absorbance mode.

### **2.3.5 Scanning electron microscope (SEM)**

In order to obtain the morphology of PU foams scanning electron microscopy was used. Firstly, specimens from PU foams were coated with a layer of gold for SEM images to avoid charging and make the material conductive. SEM photographs taken from FEI Qanta Feg 250 SEM device with 3 kV accelerating voltage. Magnification rates of images were 100x, 500x and 1000x.

### **2.3.6 Compression test**

In order to obtain the compressive properties of PU foam, compression tests were performed by using Shimadzu AGS-X universal testing machine with a 5kN load cell. Compression tests of the produced materials were carried out according to BS EN ISO 844:2009 test standard using cubic specimens ( $50\text{mm} \times 50\text{mm} \times 50\text{mm}$ ). Test speed was set to  $5 \text{ mm/min}$  and a minimum of two test specimens compressed until 85% of its original thickness.

## **3. RESULTS AND DISCUSSION**

### **3.1 Characterization of natural fibers**

#### **3.1.1 Particle size**

Nutshell flour and olive kernel flour were subjected to mesh analysis, and materials which are smaller than  $200 \mu\text{m}$  were used as a biofiber. Particle size distributions of flours are shown in Figure 2.

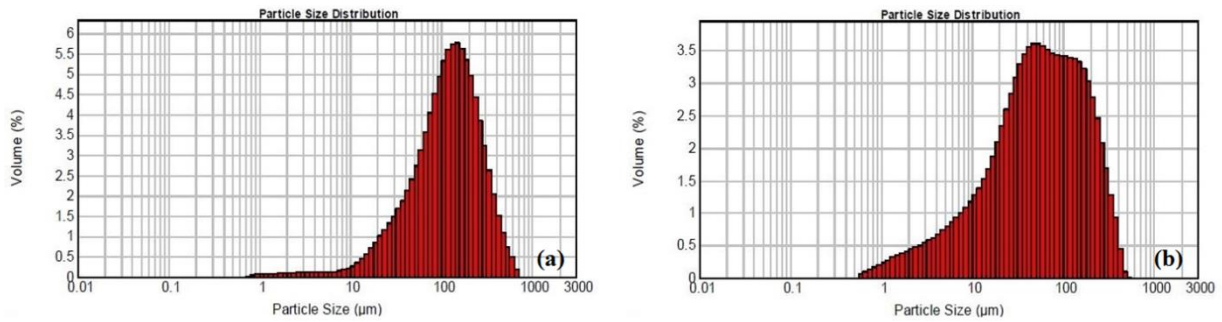


**Figure 2.** Particle size distribution of flours (a) particle size distribution of nutshell (b) particle size distribution of olive kernel

According to particle size analysis, it was determined that the particle size of nutshell is 120  $\mu\text{m}$  at  $d(0,5)$  and olive kernel is 55  $\mu\text{m}$  at  $d(0,5)$ .

### 3.1.2 X-Ray Diffraction (XRD) analysis

The X-ray spectra patterns of nutshell and olive kernel were shown in Figure 3. As seen in the figures, the intensive crystalline peak of the nutshell occurred at  $2\theta = 22.4^\circ$  and the other crystalline peak of the nutshell at  $2\theta = 15.2^\circ$  and  $2\theta = 16.6^\circ$ .

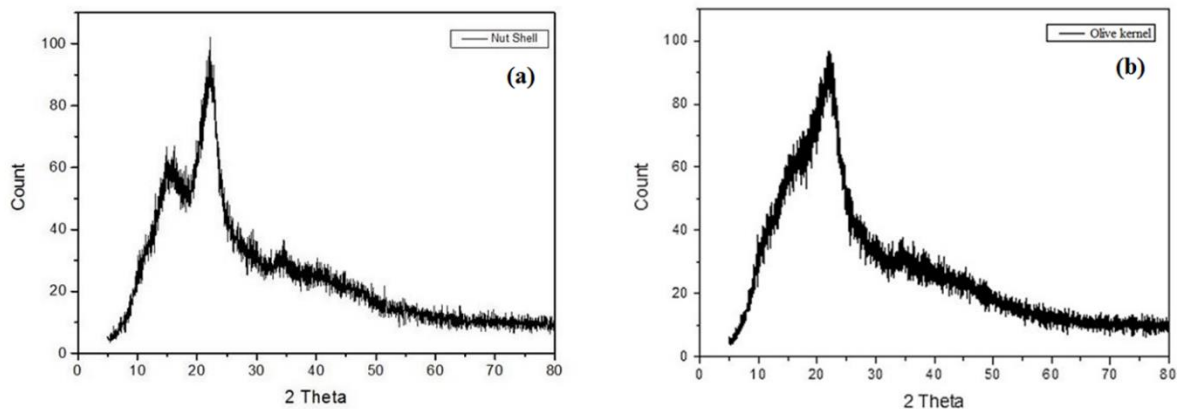


**Figure 3.** XRD analysis of natural fibers (a) XRD analysis of nutshell (b) XRD analysis of olive kernel

XRD peaks Ferula fiber had at  $15.1^\circ$ ,  $16.8^\circ$ , and  $22.2^\circ$  which is assigned to the typical diffractions of Beta phases of Cellulose-I and native cellulose [17]. Biofiber which is olive kernel peaks concerned with nutshell shows on the X-ray spectra are at  $2\theta = 15.2^\circ$  and  $2\theta = 16.6^\circ$ . Following to the, (0 1 1), (1 1 0) and (0 0 2) planes of the Cellulose-I or native cellulose solid state structure [18]. The percent crystallinity of nutshell and olive kernel was 32, 32.1 respectively. These crystallinity data are close to kapok (46%) and smaller than sisal (71%) [19]. Moreover, the crystallite size of nutshell is connected 1.6 nm and smaller than cotton (5.5 nm) and flax fiber (2.8 nm) [20].

### 3.1.3 Thermogravimetric (TGA) analysis

The TGA curves of nutshell and olive kernel are shown in Figure 4. In the temperature range between 200 and 600  $^\circ\text{C}$ , Olive kernel is presented the highest percentage weight loss (about 60%). According to information obtained from the figures, the high thermal stability was observed in the nutshell. Onset temperatures of the fibers are shown in Table 2.

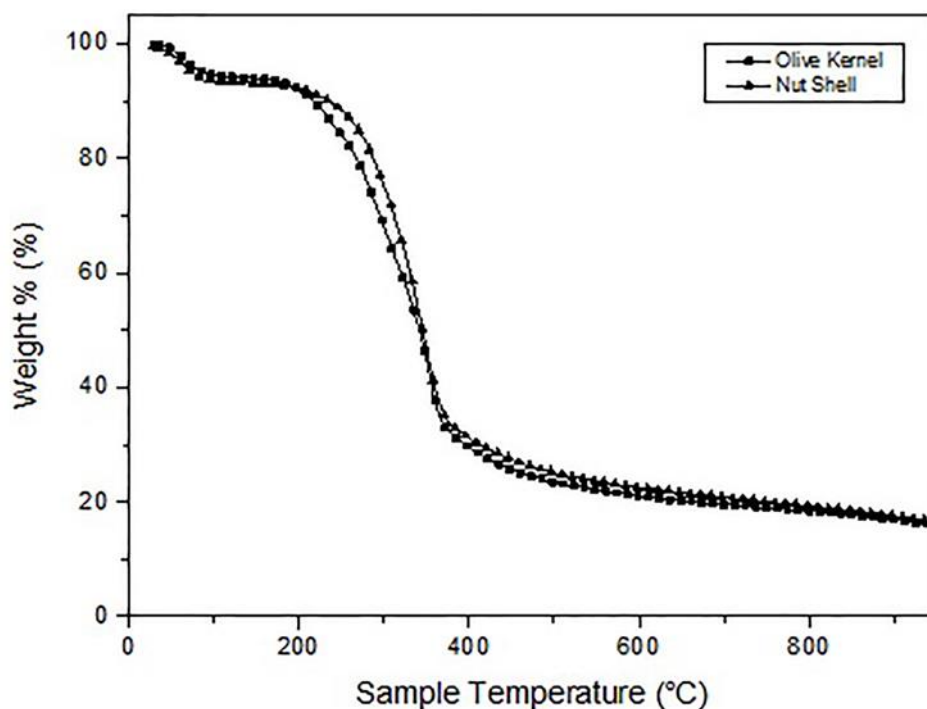


*Figure 4. TGA results for olive kernel and nutshell*

*Table 2. Onset temperatures values of nutshell and olive kernel*

	Onset	End	Step Inflection Point
<b>Nutshell</b>	<b>287.86 °C</b>	<b>375.68 °C</b>	<b>348.28 °C</b>
<b>Olive Kernel</b>	<b>281.58 °C</b>	<b>376.31 °C</b>	<b>353.18 °C</b>

### 3.1.4 Fourier Transform Infrared (FTIR) spectroscopy

FTIR spectrum of the olive kernel and nutshell are shown in Figure 5 and Figure 6. The major absorbance peaks denote characteristic peaks belonging to lignin, cellulose, and hemicellulose in lignocellulosic compounds [21].

(–OH) groups correspond to occurring peak at  $3292\text{ cm}^{-1}$  and  $3333\text{ cm}^{-1}$  [22]. The presence of OH groups in the structure is estimated to be due to cellulose contained in the olive kernel and nutshell. At  $2923\text{ cm}^{-1}$  and  $2917\text{ cm}^{-1}$  peaks –CH stretching band occurred based on the alkyl groups [23]. The C = O peak of found in hemicellulose structure is observed at  $1710\text{ cm}^{-1}$  and  $1594\text{ cm}^{-1}$ .<sup>21</sup> At  $1507\text{ cm}^{-1}$  and  $1509\text{ cm}^{-1}$  is associated to C=C stretching band. This peak was observed due to aromatic ring vibration found of in the structure of lignin. At  $1239\text{ cm}^{-1}$  and  $1235\text{ cm}^{-1}$  occurred peaks are seen due to OH bending vibration indicating the presence of phenolic group situated in the cellulose structure or ether bridges between the ring structures in the hemicellulose. At  $1032\text{ cm}^{-1}$  and  $1030\text{ cm}^{-1}$  is represented to in-plane bending of aromatic ring CH bond [22].

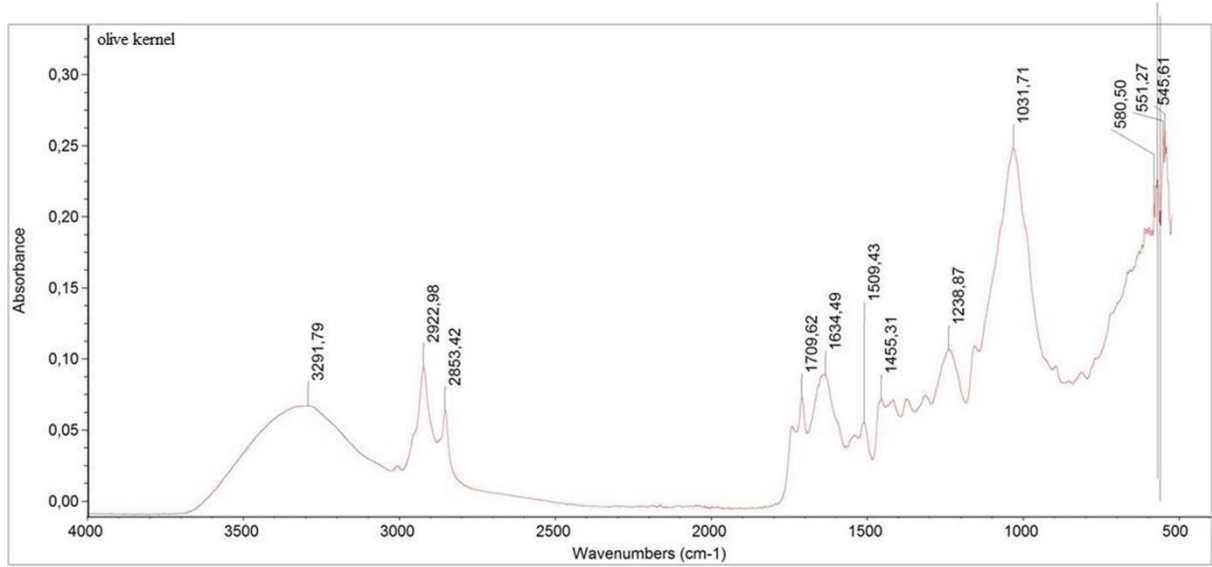


*Figure 5. FTIR spectrum for olive kernel*

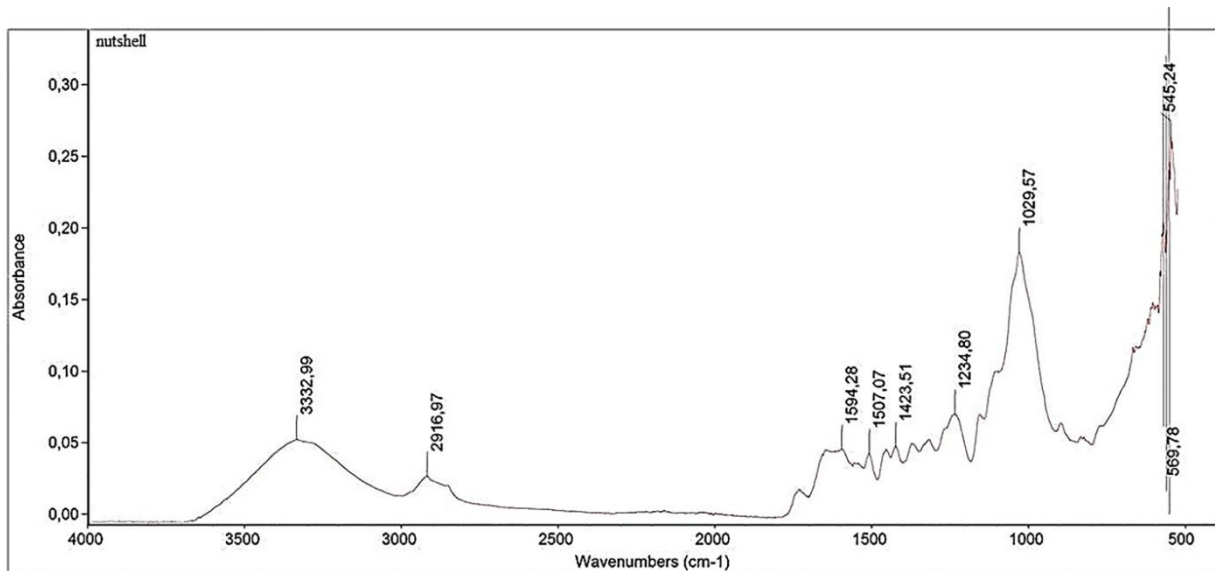


*Figure 6. FTIR spectrum for nutshell*

### 3.2. Characterization of biofiber reinforced PU composites

#### 3.2.1 Thermogravimetric (TGA) analysis

Polyurethane foam with natural fibers have different onset temperatures. The onset temperatures of the neat materials (the biofillers and the polyurethane) and PU composites at 5 wt % are shown in Table 3.

*Table 3. Onset temperatures values of all samples*

	Onset	End	Step Inflection Point
<b>Nutshell</b>	287.86 °C	375.68 °C	348.28 °C
<b>PU</b>	290.72 °C	394.46 °C	335.71 °C



<b>PU + 5% Nutshell</b>	280.80 °C	382.93 °C	338.48 °C
<b>Olive Kernel</b>	281.58 °C	376.31 °C	353.18 °C
<b>PU + 5% Olive Kernel</b>	280.30 °C	381.44 °C	338.66 °C

As expected, the natural fibers have lower onset temperatures due to easy burning characteristic of these materials. Polyurethane had a slightly higher onset temperature value. As we add the biofibers into the polyurethane matrix, we observe certain decrease in the onset temperature of the composites compared to neat PU material. This decrease was expected as it was observed that the neat biofibers had inferior thermal stability.

Figure 7 illustrates that the TGA results of the PU formed with olive kernel and nutshell contain natural fibers. The TGA curves of the synthesized polyurethane foam presents a typical decomposition in two stages between 40 and 600 °C. The major constituents of fiber are cellulose, hemi cellulose and lignin are decomposed in the regions between 250 and 480 °C [24]. The PU decomposes in the temperature range 330–400 °C, losing CO<sub>2</sub> and with a final residue of ~80%. According to their thermogravimetric/derivative thermogravimetric (TGA/DTG) results, which showed the flexible polyurethane foam containing commercial calcium carbonate (CaCO<sub>3</sub>) and illustrated that the surplus of commercial CaCO<sub>3</sub> used in industry causes the permanent deformations and damaging the standard of the final product [25].

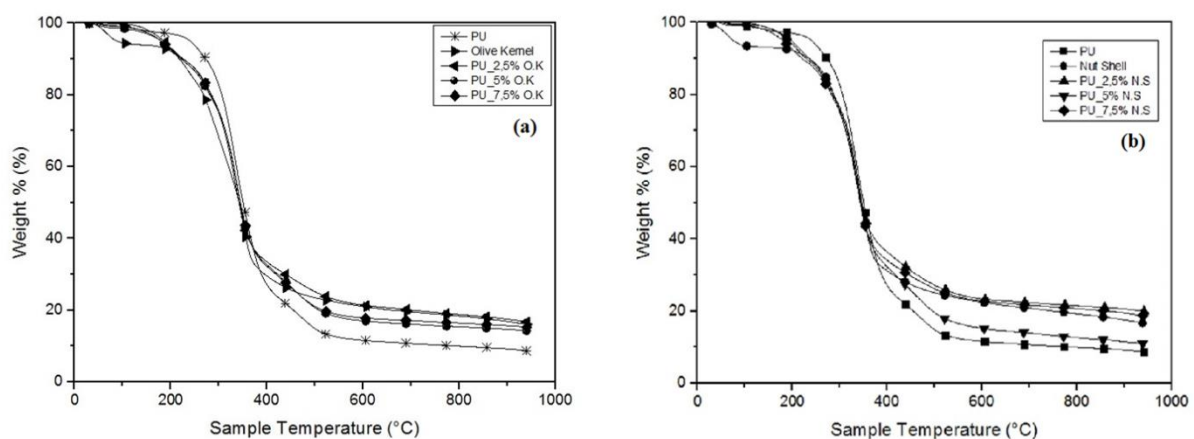


**Figure 7.** TGA results for all PU samples (a) TGA results for all PU samples with olive kernel (b) TGA results for all PU samples with nutshell

When the composites of nutshell and olive kernel are compared, it was observed that the onset temperatures were very close. Although, the fibers are mixed at low concentration, it could still affect the thermal degradation of the polyurethane matrix. To observe that there was no significant change regarding to biofiber was also an important observation.

### 3.2.2 Fourier Transform Infrared (FTIR) spectroscopy

FTIR spectrum of the pure polyurethane used as matrix is shown in Figure 8. The –NH stretching vibration band of urethane is assigned at 3319 cm<sup>-1</sup>. The band at 2924 cm<sup>-1</sup> corresponds to –CH bond. The –C=O stretching vibration band at 1709 cm<sup>-1</sup> was carboxylic acid in urethane. At 1602 cm<sup>-1</sup> is observed C–C bond in the aromatic ring. The band is occurred at 1511 cm<sup>-1</sup> due to stretching vibrations of the –NH.

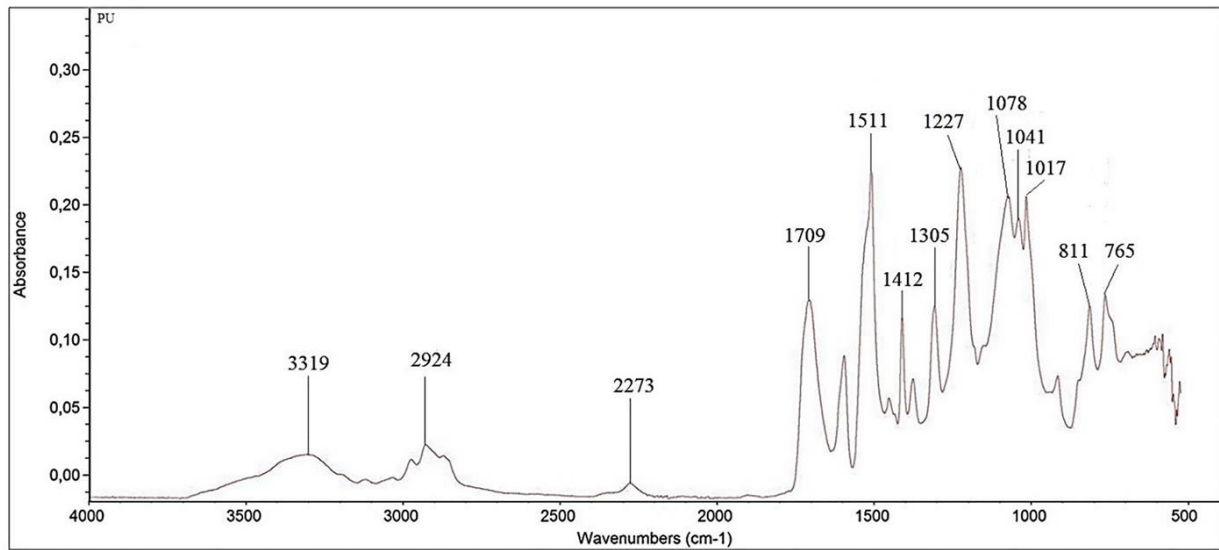


**Figure 8.** FTIR spectrum for pure PU

FTIR spectra of pure PU, olive kernel and nutshell reinforced PU foam are shown together in Figure 9. Spectrum of pure PU foam with different biofiber reinforced PU foams when compared to any shift in the peak or a new peak formation does not occur. According to this, Olive kernels and nutshell of fiber is observed that does not cause any change in the structure of the PU.

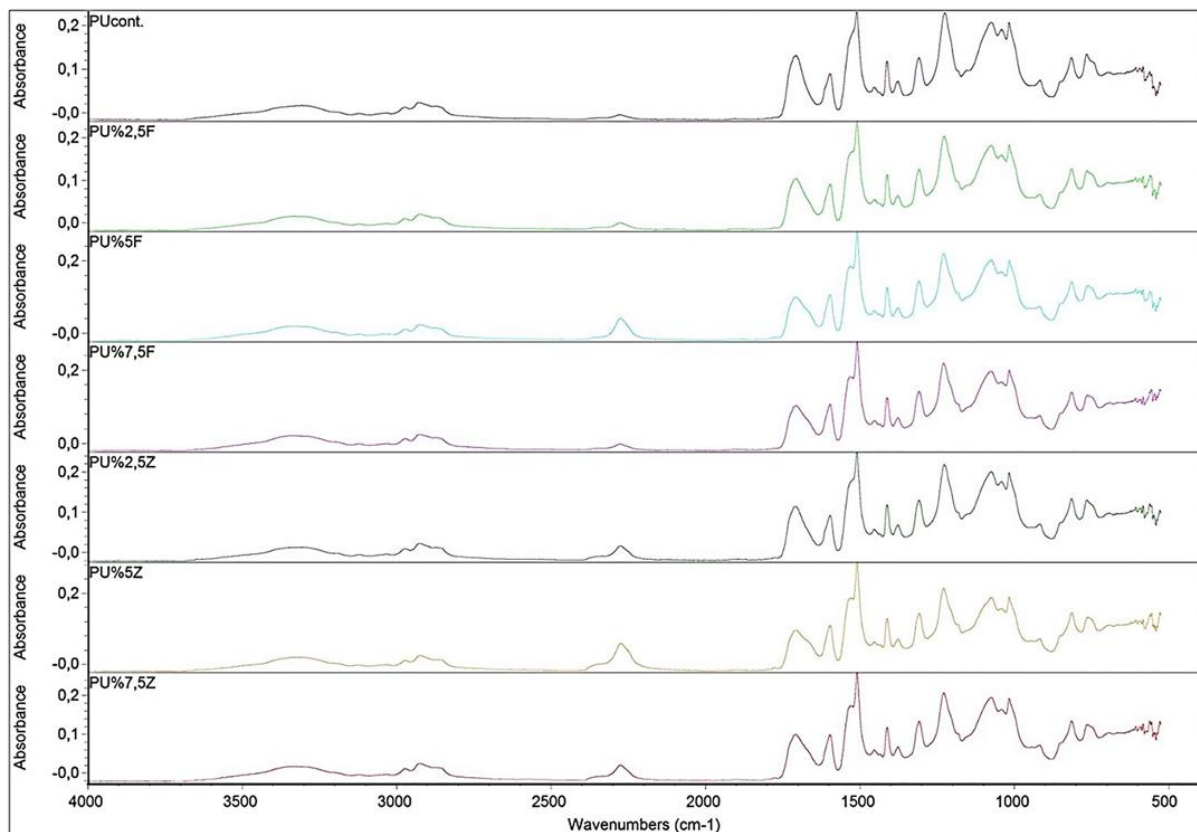


**Figure 9.** FTIR spectra of pure PU and different natural fiber reinforced PU foam

According to all these FTIR analysis results, the presence of biofiber in the foam is observed to cause adverse effect on the reaction. In spite of this negative effect, the increase in mechanical properties of biofiber reinforced of PU foam is demonstrated inspected the results of compression test in part 3.3.4.



### 3.2.3 Scanning electron microscope (SEM)

As shown in scanning electron microscopy results pure PU had uniformly distributed cells with the shape of irregular polyhedral (see Figure 10). The cells structure is closed and there is no connection between them.

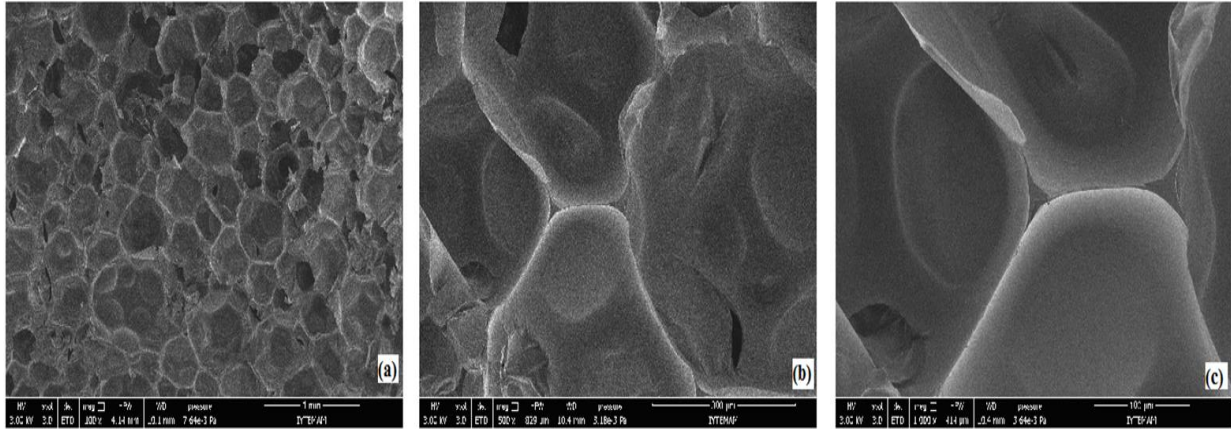


*Figure 10. SEM images of pure PU foam (a) 100x magnification (b) 500x magnification (c) 1000x magnification*

With addition of natural fibers to PU foam caused the foam to lose its characteristic polyhedral morphology [25]. Also use of fillers affected the nucleation mechanism. Natural fibers in PU foam started to growth from beginning of the nucleation points and prevented to be uniform cell structure. Distortion of the cell walls increased progressively with increasing filler concentration (see Figure 11 and Figure 12). This case can be observed clearly in nutshell filled PU foams. Although being defect of nutshell in the high concentration, olive kernel fillers did not affect morphology significantly.

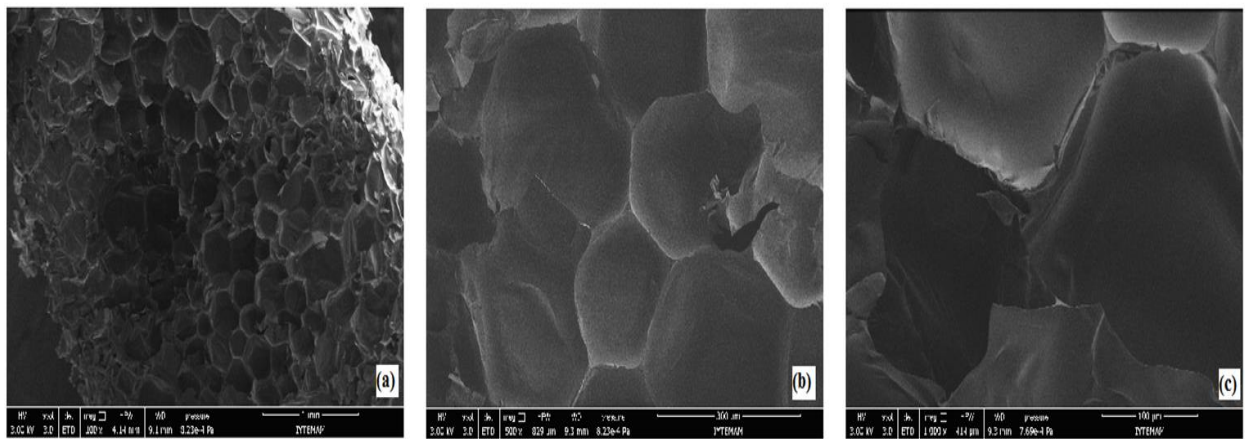


*Figure 11. SEM images of 7.5% olive kernel reinforced PU foam (a) 100x magnification (b) 500x magnification (c) 1000x magnification*

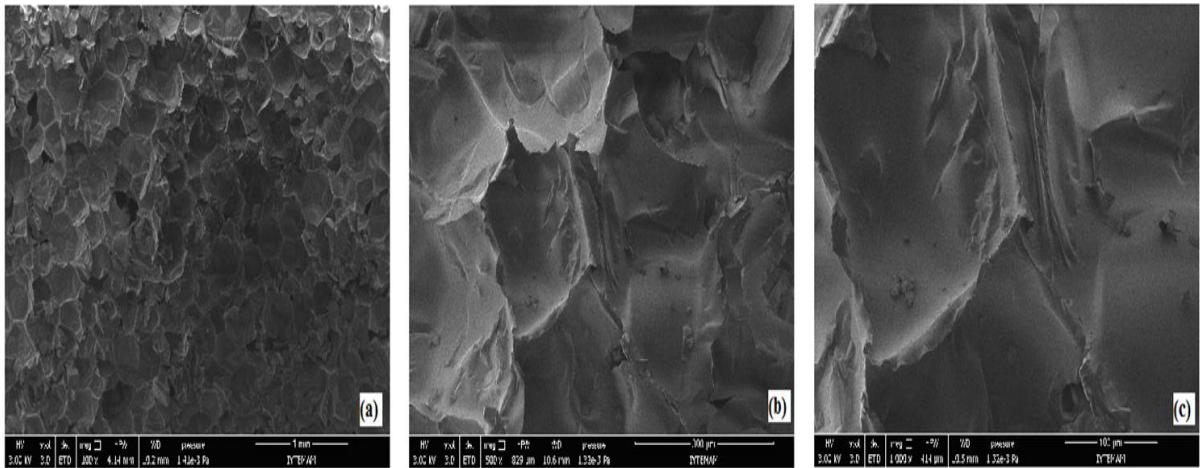


**Figure 12.** SEM images of 7.5% nutshell reinforced PU foam (a) 100x magnification (b) 500x magnification (c) 1000x magnification

### 3.2.4 Compression test

The effects of olive kernel and nutshell fibers on the mechanical properties of the PU foam were investigated. As a result of the compression test, compressive modulus and maximum compressive strength of pure PU foam, PU foam filled with olive kernel and nutshells were compared.

**Table 4.** Comparison Compressive Modulus and Maximum Compressive Strength of polyurethane foam filled with olive kernel and nutshell

Filler Concentration (%)	Nutshell		Olive Kernel	
	Compressive Modulus (MPa)	Max Compressive Strength (kPa)	Compressive Modulus (MPa)	Max Compressive Strength (kPa)
0	1,56	86,28	1,56	86,28
2,5	1,65	107,27	2,20	126,88
5	1,58	81,33	1,50	95,39
7,5	1,15	51,14	1,31	83,96

Table 4 shows while compressive modulus and max compressive strength were increasing with loading of 2.5 wt%, decreased with 5 wt% and 7.5 wt% loading ratio. The compressive strength of pure rigid foam is 86.28 kPa and compressive modulus is 1.56 MPa. Along with 2.5 wt% addition of olive kernel these parameters reach maximum value. Compressive properties for nutshell fibers filled PU foam are inferior than olive kernel filled foam. So, 2.5 wt% filling rate with olive kernel is the best formulation for compressive properties of PU foam.

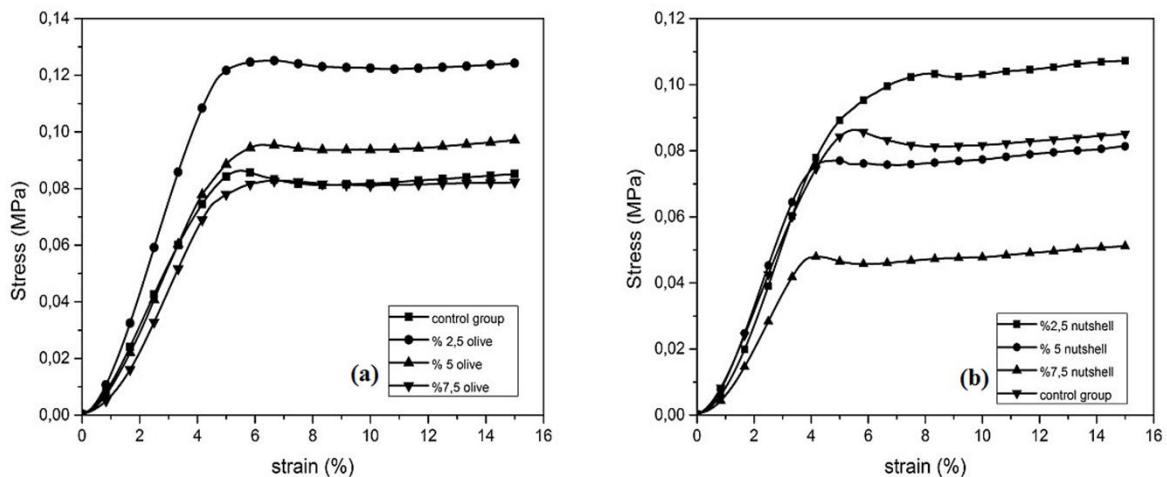


**Figure 13.** Stress–strain curves of foam samples (a) stress-strain curves for pure PU foam and filled olive kernel foam (b) stress-strain curves for pure PU foam and filled nutshell foam all PU

Typical stress-strain curves for PU foams are shown in Figure 13. As the seen in curves there is apparent decrease for 7.5wt% of nutshell filler based foams. This is because of stiffness effect of the nutshell. Also nutshell and olive kernel particles can be thought as a non-deformable filler embedded into the foam structure it would act as a defect, leading to the embrittlement of the cell walls [26]. Scanning electron micrographs show that pure PU foam has mostly spherical and equally distributed cell structure. When fillers were introduced and with increased filler rate it could be observed that foam cell structure became more distorted and less uniform distribution. At this time if there is an application of loading, bending and shrinkage of cell walls occur and results in the development of micro cracks. Therefore, foam strength extremely depends on the initiation of micro cracks and forces on their growth [27]. So it can be explained with the decreasing of foam compressive strength with crack initiation and growth.

Finally, the reason of the decreasing mechanical strength might be at high filling rate, it is difficult to gain uniformly dispersion of particles and polyol mixture. So this caused less uniform foam structure as can be seen from SEM images and decreased mechanical properties [26]. Non-uniform concentration in some regions contributed to embrittlement effect of polymer structures and cell walls became weaker. Weak cell walls could not support the foam structure under loading and cleavage of cell wall was promoted.

#### 4. CONCLUSION

In this study, it was shown that biofibers obtained from Turkish local resources could be well integrated into polyurethane foam with increasing mechanical strength. The olive kernel and nut shell is found in abundantly in Turkish natural resources and they are commonly used as biomass for heating. By this study, we have successfully demonstrated these resources could be well integrated into polymer structures making the polyurethane foam more environment friendly and more sustainable. The FTIR and TGA analysis further enhanced our analyses for composite preparation and SEM images show that polyurethane foam structure was uniformly formed with a closed cell structure.

#### CONFLICT OF INTEREST

No conflict of interest was declared by the authors

#### REFERENCES

- [1] D.K. Chattopadhyay, K.V.S.N. Raju, Structural engineering of polyurethane coatings for high performance applications, *Progress in Polymer Science*, 32 (2007) 352– 418.
- [2] M. Faruk, M. Sain, R. Farnood, Development of lignin and nanocellulose enhanced bio PU foams for automotive parts, *Journal of Polymers and the Environment*, 22 (2013) 279–288.

- [3] M. Szycher, *Szycher's Handbook of Polyurethanes*, CRC Press, Boca Raton, 2012.
- [4] D. Randall, S. Lee, *The (Huntsman) Polyurethanes Book*, John Wiley & Sons, Inc., Oxford, 2003.
- [5] C.A. Cateto, M.F. Barreiro, A.E. Rodrigues, M.N. Belgacem, Optimization of lignin oxypropylation in view of polyurethane rigid foams preparation, *Ind. Eng. Chem. Res.*, 48:5 (2009) 2583–2589.
- [6] T.U. Patro, G. Harikrishnan, A. Misra, D.V. Khakhar, Formation and characterization of polyurethane-vermiculite clay nanocomposite foams, *Polym. Eng. Sci.*, 48 (2008) 1778–1784.
- [7] Z.B. Xu, X.L. Tang, A.J. Guand, Z.P. Fang, Novel preparation and mechanical properties of rigid polyurethane foam/organoclay nanocomposites, *J. Appl. Polym. Sci.*, 106 (2007) 439–447.
- [8] C.C. Saliba, R.L. Oréfice, J.R.G. Carneiro, A.K. Duarte, W.T. Schneider, M.R.F. Fernandes, Effect of the incorporation of a novel natural inorganic short fiber on the properties of polyurethane composites, *Polym. Test.*, 24:7 (2005) 819-824.
- [9] Z. Bartczak, A.S. Argon, R.E. Cohen, M. Weinberg, Toughness mechanism in semi-crystalline polymer blends: II. High-density polyethylene toughened with calcium carbonate filler particles, *Polymer* 40:9 (1999) 2347- 2365.
- [10] I. Banik, M. Sain, Water blown soy polyol-based polyurethane foams of different rigidities, *J. Reinf. Plast. Compos.*, 27 (2008) 357-373.
- [11] D. Rusu, S. A. E. Boyer, M. F. Lacrampe, P. Krawczak, *Handbook of Bioplastics and Biocomposites Engineering Applications*, Massachusetts, (2011) 427-428.
- [12] A. Prociak, M. Kurańska, E. Malewska, L. Szczepkowski, M. Zieleniewska, J. Ryszkowska, J. Ficoń, A. Rzasa, Biobased polyurethane foams modified with natural fillers, *Polimery*, 60:09 (2015) 592-599.
- [13] M. Kurańska, A. Prociak, Porous polyurethane composites with natural fibres, *Composites Science and Technology*, 72 (2012) 299-304.
- [14] M. Kurańska, A. Prociak, A. Mikelis, C. Ugis, Porous polyurethane composites based on bio-components, *Composites Science and Technology*, 75 (2013) 70–76.
- [15] R. Gu, M.M. Sain, Effects of wood fiber and microclay on the performance of soil based PU foam, *J. Polym. Environ.*, 21 (2013) 30–38.
- [16] R. Gu, M.M. Sain, S.K. Konar, A feasibility study of polyurethane composite foam with added hardwood pulp, *Industrial Crops and Products*, 42 (2013) 273– 279.
- [17] Y. Seki, M. Sarikanat, K. Sever, C. Durmuşkahya, Extraction and properties of ferula communis (Chakshir) fibers as novel reinforcement for composites materials composites, *Part B: Engineering*, 44:1 (2013) 517–523.
- [18] D. Treheux, B. Kechaou, M. Salvia, B. Beaugiraud, D. Juve, Z. Fakhfakh, Mechanical and dielectric characterization of hemp fiber reinforced polypropylene (HFRPP) by dry impregnation process, *Express Polym. Lett.*, 4:3 (2010) 171–82.
- [19] L.Y. Mwaikambo, M.P. Ansell, Chemical modification of hemp, sisal, jute, and kapok fibers by alkalization, *J. Appl. Polym. Sci.*, 84:12 (2002) 2222–2234.
- [20] N. Reddy, Y. Yang, Structure and properties of high quality natural cellulose fibers from cornstalks, *Polymer*, 46:15 (2005) 5494–500.

- [21] H. Essabir, M. El Achaby, H. El Moukhtar, R. Bouhfid, A. Qaiss, Morphological, structural, thermal and tensile properties of high density polyethylene composites reinforced with treated argan nut shell particles, *Journal of Bionic Engineering*, 12 (2015) 129–141.
- [22] O.A. Ioannidou, A.A. Zabaniotou, G.G. Stavropoulos, M.A. Islam, T.A. Albanis, Preparation of activated carbons from agricultural residues for pesticide adsorption, *Chemosphere*, 80:11 (2010) 1328–1336.
- [23] Y. Peng, S. Wu, The structural and thermal characteristics of wheat straw hemicellulose, *Journal of Analytical and Applied Pyrolysis*, 88 (2010) 134–139.
- [24] S. Mishra, A.K. Mohanty, L.T. Drzal, M. Misra, G. Hinrichsen, A review on pineapple leaf fibers, sisal fibers and their biocomposites, *Macro. Mater. Eng.*, 289 (2004) 955–74.
- [25] S. Sá e Sant'Anna, D. Arlindo de Souza, D. Marques de Araujo, C. Cornélio de Freitas, M.I. Yoshida, Physico-chemical analysis of flexible polyurethane foams containing commercial calcium carbonate, *Material Research*, 11:4 (2008) 433 – 438.
- [26] H. Fan, A. Tekei, G.J. Suppes, F. Hsieh, Properties of biobased rigid polyurethane foams reinforced with fillers: Microspheres and Nanoclay, *International Journal of Polymer Science*, 2012 (2012) 1-8.
- [27] M.A. Mosiewicki, G.A. Dell'Arciprete, M.I. Aranguren, N.E. Marcovich, Polyurethane foams obtained from castor oil-based polyol and filled with wood flour, *Journal of Composite Materials*, 43:25 (2009) 3057-3072.